Nat Hazards
DOI 10.1007/s11069-016-2349-2

ORIGINAL PAPER

Coastal boulder deposits attesting to large wave impacts on the Mediterranean coast of Egypt

Majid Shah-Hosseini[1] · Amr Saleem[2] · Abdel-Moneim A. Mahmoud[3] · Christophe Morhange[1]

Received: 25 October 2015 / Accepted: 2 May 2016

Abstract Coastal boulder accumulations are documented along the Mediterranean coast of Egypt between Alexandria and Marsa Matrouh at four distinct sites. The spatial distribution and dimensions of 116 medium to large boulders were documented along four representative coastal profiles. Boulders weigh up to 23 metric tons and are located up to 40 m from the shoreline. Geomorphologic features, morphometric properties and the presence of attached marine organisms attest that the boulders are detached and transported from original subtidal or intertidal settings by the impact of unusually large waves. Adapted hydrodynamic models were applied to evaluate the height of the transporting waves. Our result shows that largest boulders could be transported by tsunami waves of 2.6 m or storm wave of about 10 m in height. Radiocarbon dating was performed on fixed marine gastropod (*Vermetidae* and *Dendropoma*) shells found on four representative large boulders. A calibrated age from the easternmost site is roughly coincident to the well-known tsunami of 1303 AD in the eastern Mediterranean. Three other calibrated ages correspond to a period ranging from the eighteenth century AD to present. A large tsunami like the event of 1303 AD would have been able to transport all of the studied boulders. However, radiocarbon ages and morphological properties such as freshly broken edges and surfaces suggest younger ages for the majority of boulders. Since there have been no large, post-1303 AD tsunamis reported, we suggest that the majority, if not all, of the boulders were most likely deposited by multiple intense storms. According to the wave height model, storms with wave heights exceeding 9 m at their breaking point probably occur about once every 100 years. A relationship between the boulder deposits and the high storm frequency that characterized the little ice age in the Mediterranean Sea is plausible. This study emphasizes the potential hazard of large waves on this part of the Mediterranean coast of Egypt.

✉ Majid Shah-Hosseini
shmajid@gmail.com

[1] CNRS, IRD, CEREGE UM34, Aix-Marseille Université, 13545 Aix en Provence, France

[2] Department of Geography, Faculty of Arts, Ain-Shams University, Cairo, Egypt

[3] Department of Geology and Biology, Faculty of Education, Ain-Shams University, Cairo, Egypt

Published online: 25 May 2016

Keywords Boulder deposits · Coastal hazard · Mediterranean coast of Egypt · Tsunami · Storm

1 Introduction

Coastal hazards are among major environmental issues in many parts of the world. A large portion of the world's population lives in coastal areas. With the expansion of human settlements and infrastructure, coastal risk assessments and preparation are critical for sustainable development. Inundation by large waves is a major hazard that threatens many coasts with intense storms and tsunamis being the main sources of high-energy, low-frequency marine flooding. The impact of exceptionally large waves on a coast can be recorded in the geomorphological and sedimentological archive as erosional and/or depositional features. Along rocky coasts, the detachment and landward displacement of mega-clasts is a known indicator of the impact of high-energy waves (Dawson 1994, Nott 1997, 2000, 2003; Noormets et al. 2004; Goff et al. 2004, 2006; Morton et al. 2006; Goto et al. 2007; Imamura et al. 2008; Stewart and Morhange 2009; Barbano et al. 2010; Etienne and Paris 2010; Nandasena et al. 2011, 2013; Engel and May 2012; Shah-hosseini et al. 2011, 2013). In the Mediterranean, as well as many other coasts in the world, accumulations of coastal displaced boulders have been related to tsunami or storm impacts in numerous studies (e.g. Mastronuzzi and Sansò 2000, 2004; Morhange et al. 2006; Mastronuzzi et al. 2007; Scicchitano et al. 2007; Vött et al. 2010; Barbano et al. 2010; Maouche et al. 2009; Vacchi et al. 2012; Shah-Hosseini et al. 2013; Raji et al. 2015; Biolchi et al. 2016). The Mediterranean basin is situated in a tectonically active setting with significant volcanism and a long record of historical earthquakes and tsunamis (Guidoboni et al. 1994; Papadopoulos and Fokaefs 2005; Salamon et al. 2007; Stewart and Morhange 2009; Anzidei et al. 2014; Papadopoulos et al. 2014). Numerous anomalous coastal deposits have been studied in the Mediterranean. In many cases, high-energy deposits have been related to historical or prehistorical tsunamis particularly in the eastern Mediterranean. However, in the southern coast of Mediterranean, coastal hazard studies are relatively rare. Although historically less well known, the tsunami hazard potential is high along the African coast of the Mediterranean due mainly to the proximity of major active faults. Roman historian, Amiano Marcellino has described the tsunami of 365 AD that destroyed Alexandria port and killed about 50,000 people (Mastronuzzi et al. 2013). Another large tsunami in 1303 struck Alexandria, it damaged a large part of the city wall and the famous lighthouse (El-Sayed et al. 2000; Ambraseys 2009). On the Egyptian coast, the presence of displaced mega-clasts is noted around Alam-El-Rum (Torab and Dalal 2015). Intense storms are also an important source of catastrophic large waves in the Mediterranean (e.g. Lionello et al. 2006; Sabatier et al. 2012), and displaced boulders have been shown to be related to extreme storm events in several studies (e.g. Barbano et al. 2010; Paris et al. 2011; Shah-hosseini et al. 2013).

Egypt has a long stretch of coastline along the Mediterranean Sea. Around 35 million people in Egypt, about 45 % of the country's population are living in areas below 10 m above sea level and prone to coastal inundation. The population density, particularly in Nile delta, is high and reaches 250–1000 people/km^2 (NASA's Earth Observing System Data and Information System—EOSDIS). Important infrastructure is also concentrated in these coastal areas. The history of past events is a key to understanding the hazard potential

for a given coast. Historical records of catastrophic events in the eastern Mediterranean are long and relatively complete compared to other parts of the world (e.g. Guidoboni et al. 1994; Soloviev et al. 2000; Papadopoulos and Fokaefs 2005; Salamon et al. 2007; Papadopoulos et al. 2014). However, early historical records for the coast of Egypt are considered relatively incomplete because of the lack of population in areas other than big ancient cities such as Alexandria. Instrumental records are only available for less than a century (e.g. Frihy 2001). Considering these limitations, geomorphological studies are essential for the identification and interpretation of past events. This study examines displaced coastal boulders as evidence for large wave impacts along a stretch of the Mediterranean coast of Egypt. Using hydrodynamic models, we evaluate wave heights that would have been able to dislodge and transport boulders to their present position; furthermore, we discuss possible sources for extreme waves. This study contributes to a better understanding of the vulnerability of the Mediterranean coast of Egypt to natural hazards. It also increases our knowledge about the nature and frequency of extreme wave impacts on the eastern Mediterranean coast.

2 Study area

2.1 Tectonic setting

The eastern Mediterranean basin is situated at the convergence zone of the Eurasian and African-Arabian tectonic plates where the Tethys oceanic lithosphere has been

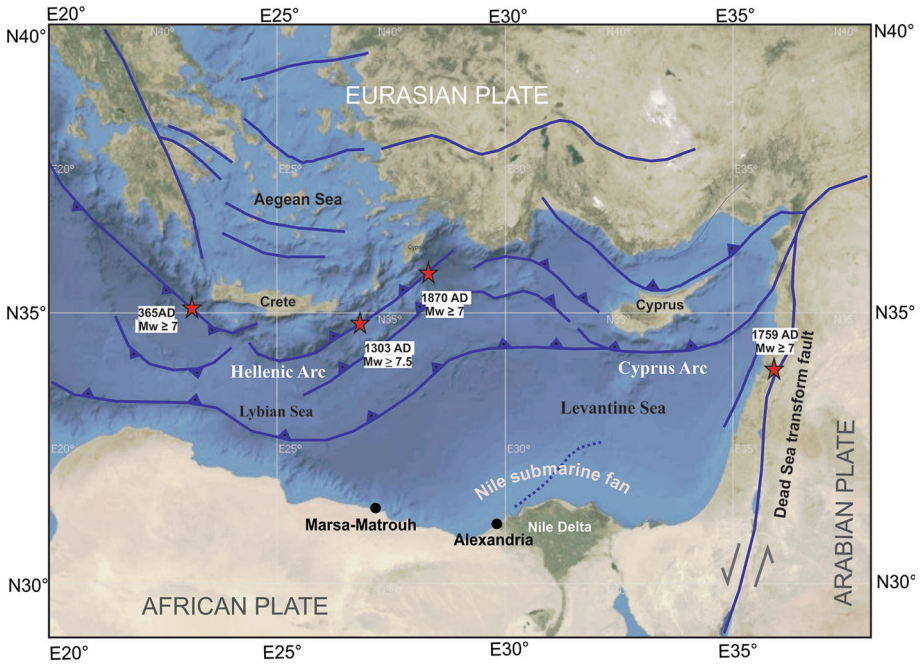

Fig. 1 Main geological and structural features of the eastern Mediterranean and approximate source of historical tsunamis reported in coast of Egypt

progressively subducted beneath the Eurasian continental lithosphere (e.g. McKenzie 1972; Anzidei et al. 2014). A complex subduction system has been formed in eastern Mediterranean as a result of this tectonic activity. The Hellenic and Cyprus arc subduction systems are major active margins in the region (Fig. 1), numerous large earthquakes reported from these sources. Furthermore, destructive historical tsunamis in the eastern Mediterranean are mainly related to these sources (Ambraseys 2009; Papadopoulos et al. 2014). Volcanic activity in the Tyrrhenian and Aegean seas is also known as a potential tsunamigenic source in the eastern Mediterranean (Goodman-Tchernov et al. 2009; Mastronuzzi 2010; Morhange et al. 2014) with the steep slopes of the Levant passive margin and the Nile submarine fan also prone to submarine slumps that can trigger tsunamis (Salamon et al. 2007). Therefore, the eastern Mediterranean basin is an area prone to large earthquakes and tsunamis.

2.2 Coastal geomorphology and wave climate

The study area is a section of coast approximately 130 km long between Ras-el-Hekma to the east and Marsa Matrouh to the west (Fig. 2). This part of the coast has many tourist facilities and large national development projects. The coastal geomorphology is characterized by alternating rocky headlands and synclinal beaches. The lithology of the rocky coast consists of Pleistocene–Pliocene and Miocene oolitic limestone formations (Embabi 2004). Boulder accumulations comprised of local lithology are mainly found on the lower parts of the rocky coast up to 2 m above mean sea level.

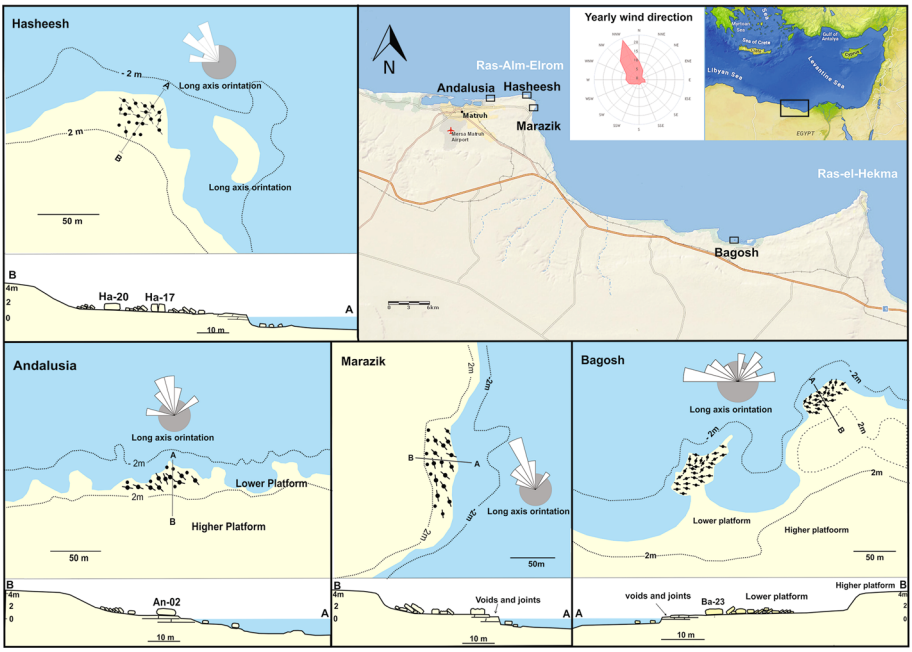

Fig. 2 Location map and profiles of studied boulder deposits, long-axis orientation of boulders also shown as *rose diagrams*. Wind direction distribution in Marsa Matrouh is presented for the period of 2001–2015 (wind data from www.windfinder.com)

The wave climate of the Mediterranean is seasonal and highly influenced by the North Atlantic oscillation system. Wave height measurements of Alexandria and Marsa Matrouh have been recorded since the 1970s, but a continuous record only covers the past decade. Observations of the wind-induced wave regime and swells to the west of Alexandria show that 75 % of the waves reach the coast from a WNW–NNW direction. For more than 50 % of the year, wave heights range between 0.5 and 1.5 m and wave period between 5 and 7 s. Wave periods are in the range of 6–9 s for NW waves and 5–8 s for NE waves for 60 % of the time, reaching a maximum of 14 s (Naffaa et al. 1991; Iskander 2013). The wind records from Marsa Matrouh airport with continuous recording between 2001 and 2015, showing that for 49 % of the time the wind direction is N to NW. Average wind speed is lowest in November (18.5 km/h) and highest from February to April (24 km/h) (data from www.windfinder.com). Storminess usually occurs during winter from mid-October to March. In general, 16 storms occur each year with at least seven being fairly strong (Iskander, 2013). A maximum wind speed of 63 knots (116 km/h) recorded during the Baqi-Kasem spring storm (Eissa 1994). Iskander (2013) reported an increasing trend in the significant wave height from 1985 onwards at a rate of 2.6–2.9 cm/year. Extreme storm surge and wave height data are not available in the study area due to a lack of measurements and documentation, but by extrapolation of the existing data, the maximum significant wave height is calculated to be about 4 m for an annual return period, 7.6 m for 50 years and 8.1 m for 100 years (Iskander 2013).

3 Methods

3.1 Boulder characteristics

Four field campaigns were carried out from May 2012 to June 2013 to document the boulder deposits. Thousands of boulder-sized transported clasts were observed along the studied coastline. For this study, we recorded morphometric characteristics of medium to very coarse boulders (0.5–4 m in length according to classification of Blair and McPherson 1999). Dimensions and distance from the shoreline of each boulder were directly measured in the field. A total station was used for profiling the coastal platform in a shore-normal transect for each boulder site. The volume of each boulder was calculated by multiplying the length (a axis), width (b axis) and thickness (c axis) of each clast. Hoffmeister et al. (2014) show that irregularity in the shape of boulders can lead to a systematic overestimation of volume. To reduce potential volume overestimation, we applied a mean value of each axis by averaging the maximum and minimum measurements. This correction reduced the calculated volume by about 25 % of the maximum value. The density of carbonate rocks was measured by the volumetric method on fragments from four different boulders as 2.6 g/cm^3. The mass (weight) of each boulder was calculated by multiplying the volume by the density. Orientation of the long axis of boulders was measured using a geological compass. Micro-scale geomorphological features and biological attachments were documented in order to help determine the pre-transport settings of boulders and their age. The distance from the shoreline was directly measured following the methodology proposed by Mastronuzzi and Sansò (2004).

3.2 Height of transporting waves

We apply adapted hydrodynamic models to evaluate the height of the waves capable of dislocating boulders from their original positions. Nott's (1997, 2000, 2003) model takes into account boulder axis dimensions and the pre-transport setting in order to calculate tsunami or storm wave heights. Three possible pre-transport settings are assumed: subaerial, submerged and joint bounded. Nott's equations have frequently been applied to calculate wave heights capable of initiating boulder transport (e.g. Mastronuzzi and Sansò 2004; Mastronuzzi et al. 2006; Maouche et al. 2009; Scicchitano et al. 2007; Barbano et al. 2010). However, the accuracy of Nott's model in different coastal settings has been debated in several studies (e.g. Pignatelli et al. 2009; Benner et al. 2010; Switzer and Burston 2010; Nandasena et al. 2011). Considering the coastal setting, we adopted two modifications to Nott's original equations: Pignatelli et al. (2009) for joint-bounded and Benner et al. (2010) for submerged and subaerial pre-transport settings. As stated by Pignatelli et al. (2009), for a rectangular joint-bounded boulder on the rim of a rocky shore, a wave impacts the smaller axis instead of the long one as it is stated in the original Nott equation. As this setting is observed in the study area, we assume that Pignatelli's model is more realistic. In the case of a submerged pre-transport setting, Benner et al. (2010) argued that the length of the lever arm and acceleration of the water around boulders are neglected in Nott's equations. They also noted that the coefficient of lift is 1 for cuboid and 2 for prismatic boulders. Considering the coastal geomorphology and boulder settings at our study site, the following equations were used:

For joint-bounded pre-setting (Pignatelli et al. 2009):

$$\mathrm{HT} \geq [0.5c\,(\rho S - \rho w/\rho w)]/CL$$
$$\mathrm{HS} \geq [2c\,(\rho S - \rho w/\rho w)]/CL$$

And for a submerged and subaerial boulder pre-setting (Benner et al. 2010):

$$\mathrm{Ht} \geq [0.5bc[b\,(\rho s - \rho w)\,/\rho w - \rho s\mathrm{Cm\ddot{u}c}/(\rho w g)]]/[\mathrm{CD}c2 + \mathrm{CL}b2]$$
$$\mathrm{Hs} \geq [2bc[b\,(\rho s - \rho w)\,/\rho w - \rho s\mathrm{Cm\ddot{u}c}/(\rho w g)]]/[\mathrm{CD}c2 + \mathrm{CL}b2]$$

where HT is the tsunami wave height and HS is the storm wave height at the break point. b and c are, respectively, the medium and short axes of the boulder, ρw is sea water density, ρs is boulder density, CD is the drag coefficient (= 2), CL is the lift coefficient (= 0.178), Cm is the mass coefficient (= 1), ü is the flow acceleration (= 1 m/s2) and g is the gravitational acceleration (= 9.81 m/s2).

4 Results

This study focused on four boulder accumulation sites located to the east of Marsa Matrouh. Sites are named after nearby localities as Baghosh, Marazik, Hasheesh and Andalusia, respectively from east to west. At all study sites, a lower rock (less than 2 m high) and a higher rock (more than 2 m high) platform are recognizable (Fig. 2). A total of 116 medium to very coarse boulders were documented for hydrodynamic calculations. At all sites, boulders were commonly accumulated in imbricated clusters, although some isolated large boulders were found. Since the result of hydrodynamic calculations is dependent on the pre-transport settings, the most likely pre-transport position of each

boulder was determined based on its shape, micro-morphologic features and attached marine organisms. A rectangular shape, freshly broken surfaces together with supratidal micro-karstic erosion on a surface suggested that the boulder was carved out from the edge of rocky platform and hence a joint-bounded pre-setting was used. Rounded edges and the presence of marine bio-incrustations on all surfaces of a boulder suggested a submerged pre-setting.

4.1 Boulder sites

Baghosh: this section of the coast is situated about 220 km west of Alexandria and 40 km east of Marsa Matrouh (Fig. 2). The morphology of the coast consists of low-lying rocky shores separated by sandy beaches. Fifty-two medium to very coarse boulders were documented at this site. Boulders were generally grouped in imbricated clusters on the lower part of the coastal platform to a maximum distance of 30 m from shoreline. A cluster of boulders was also found on a small tombolo (Fig. 2). In this section, about 50 % of boulders were classified as coarse and very coarse. The morphometric characteristics of the very coarse boulders with an axis longer than 2 m are listed in Table 1. Rectangular shapes and sharp edges on most of the medium and large boulders along with micro-karstic solution on the surface of most of the large boulders suggest that they were detached and transported from an original setting on the edge of the rocky platform. The rectangular pattern and empty sockets on the edge of the rocky platform are in favour of a joint-bounded pre-setting for most boulders. Marine bio-incrustations, namely *Vermetidae* and *Dendropoma* fixed gastropods, are found on different surfaces of some of the large boulders including the largest in this site (Ba-23). The latter is 3.2 m long and estimated to weigh more than 18 metric tons. This boulder is considered to have been transported from a submerged original setting to a distance of 8 m from the shoreline (Fig. 3-a). The long axis of the majority of boulders (about 70 %) is oriented in E–W direction. This trend is nearly parallel to the direction of the coastline and roughly perpendicular to the direction of prevailing winds from the N–NW.

Marazik: this site is situated about 10 km to the east of Marsa Matrouh on a rocky promontory (Fig. 2). Boulders are clustered on a lower rock platform that stretches in a N–S direction with an average elevation of 1.7 m above sea level. Thirty-two medium to very coarse boulders were documented in this site. Boulders are found at a maximum distance of 30 m and an elevation of nearly 2 m from the shoreline. The landward limit of the boulder field is marked by a rise in elevation of the rocky platform. Boulders can be divided into two groups according to their pre-transport setting. Rectangular shapes of several large boulders match joint-bounded sockets on the edge of the platform (Fig. 3-b). Supratidal karstic erosional pools on the surface of boulders also attest to detachment from the edge of the rocky platform. Another group of clustered boulders contains marine bio-incrustations in all surfaces that attest to their submerged pre-transport setting. Morphometric characteristics of the very large boulders with an axis longer than 2 m are listed in Table 1. At this site, the long axis of about 80 % of the boulders is oriented to the N–NW. This trend is generally parallel to the direction of the coastline and also prevailing winds.

Hasheesh: this boulder site is found at northern end of a promontory rocky platform named Ras-Alm-Elrom (Fig. 2). Thirty medium to very coarse boulders were documented at this site. Most boulders are in imbricated clusters up to 40 m from the shoreline where the elevation of rocky platform rises. A very coarse boulder (Ha-20) estimated to weigh more than 14 metric tons with attached marine bio-incrustations is found at a distance of 40 m from the shoreline. Another large rectangular boulder weighing about 6.7 tons (Ha-17) is

Table 1 Morphometric properties of very coarse boulders (a axis ≥ 2 m) and calculated storm (Hs) and tsunami (Ht) wave heights. Ba: Baghosh, Mr: Marazik, Ha: Hasheesh, An: Andalusia

Boulder no.	Mean a axis (m)	Mean b axis (m)	Mean c axis (m)	Volume (m^3)	Mass (t)	Distance from shoreline (m)	Ht (m)	Hs (m)
Submerged pre-transport setting								
Ba-23	3.2	2.2	1.02	7	18.3	8	1.6	6.4
Mr-23	3.2	2.8	0.5	4.5	11.6	20	2.0	7.9
Mr-24	2.9	2.6	0.5	3.8	9.8	25	1.9	7.6
Mr-25	3.7	2	0.4	3.0	7.7	27	1.5	6.0
Mr-26	3.1	1.3	0.6	2.4	6.3	29	1.0	4.2
Mr-27	2.7	2.6	0.7	4.9	12.8	25	2.1	8.6
Ha-17	1.8	1.25	1.15	2.6	6.7	12	0.6	2.5
Ha-18	2.35	1.4	0.5	1.6	4.3	14	1.2	4.7
Ha-19	3	2	0.5	3.0	7.8	18	1.6	6.5
Ha-20	2.5	1.5	1.5	5.6	14.6	40	0.7	2.8
An-01	2.5	1.5	1.5	5.6	14.6	40	0.7	2.8
An-02	3.6	3.5	0.7	8.8	22.9	6	2.6	10.4
An-04	2.2	2	0.47	2.1	5.4	1	1.6	6.4
An-06	2	0.9	0.54	1	2.5	1	0.6	2.5
Joint-bounded pre-transport setting								
Ba-01	2.5	2.3	0.45	2.6	6.7	10	1.9	7.7
Ba-03	2.4	1.4	0.32	1.1	2.8	10	1.4	5.5
Ba-04	2	0.7	0.35	0.5	1.3	10	1.5	6.0
Ba-05	2.1	1.1	0.47	1.1	2.8	10	2.0	8.0
Ba-07	2	1.7	0.24	0.8	2.1	10	1.0	4.1
Ba-08	2.6	1	0.34	0.9	2.3	12	1.5	5.8
Ba-16	2.1	0.85	0.52	0.9	2.4	12	2.2	8.9
Ba-17	2.4	0.65	0.47	0.7	1.9	12	2.0	8.0
Ba-18	2	0.97	0.42	0.8	2.1	12	1.8	7.2
Ba-24	2.2	1.6	0.44	1.5	4.0	8	1.9	7.5
Ba-26	2.4	1.5	0.6	2.2	5.6	8	2.6	10.3
Ba-27	3	2.2	0.6	4	10.3	8	2.6	10.3
Ba-28	2.55	1.4	0.22	0.8	2.0	22	0.9	3.8
Ba-30	2.2	1.5	0.4	1.3	3.4	22	1.7	6.9
Ba-42	2.5	1.5	0.24	0.9	2.3	18.5	1.0	4.1
Ba-45	1.9	1.1	0.3	0.6	1.6	26.5	1.3	5.1
Mr-05	2	1.6	0.3	1.0	2.5	28	1.3	5.1
Mr-20	3	2.03	0.4	2.4	6.3	7	1.7	6.9
Mr-21	2.8	1.5	0.6	2.5	6.6	11.5	2.6	10.3
Mr-22	2.5	1.65	0.31	1.3	3.3	7	1.3	5.3

found broken into two parts at a distance of 12 m from the shoreline. Sharp edges and the fresh surfaces of this boulder suggest a turbulent and recent emplacement (Fig. 3-c). All four very large boulders from this site are considered to have been transported from a submerged original position because they have attached subtidal marine molluscs

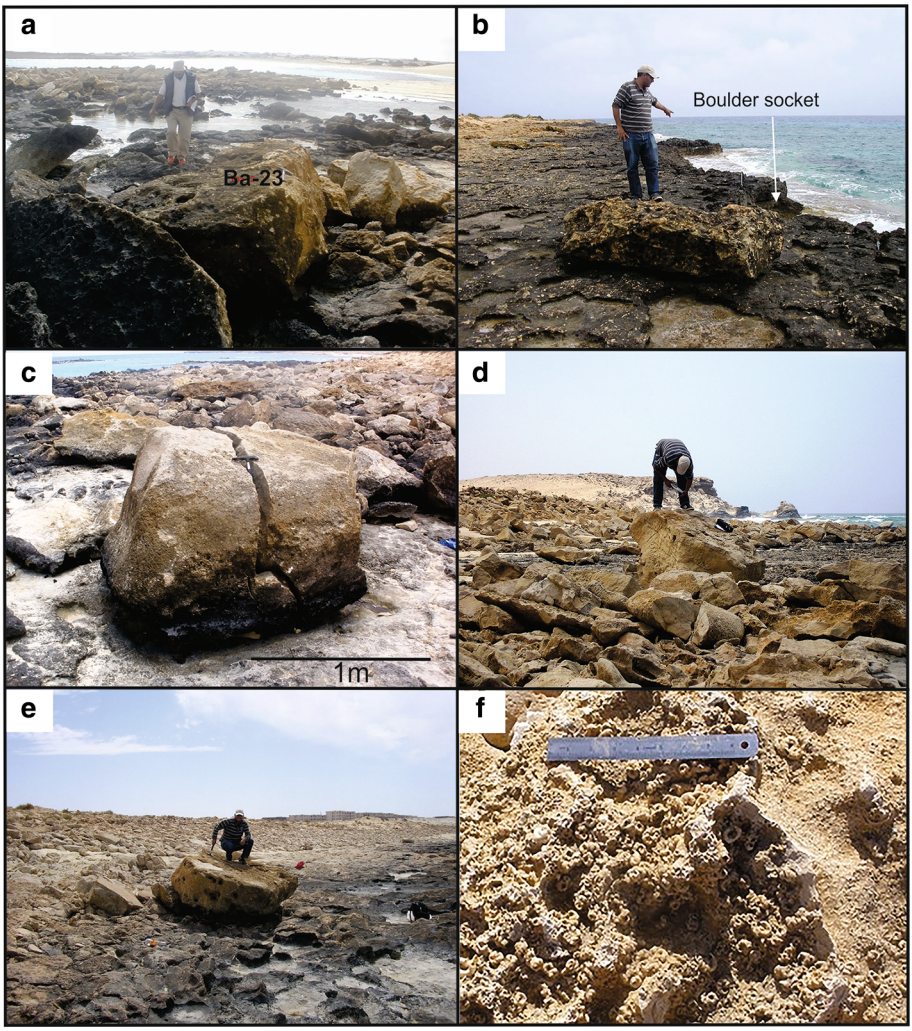

Fig. 3 **a** Boulder field in Baghosh, Ba-23, is visible in the foreground. **b** Large joint-bounded boulder in Marazik, *arrow* shows boulder's socket at the edge of the shore platform. **c** A large broken boulder in Hasheesh (Ha-17), the fresh breakage surface suggests a turbulent and recent displacement. **d** Imbricated medium boulders in Hasheesh, many medium to large boulders show sharp edges and fresh surfaces. **e** A large boulder (An-02 in Andalusia), imbricated medium boulders are visible in background. **f** Marine fixed gastropod *Vermetidae* on the surface of a boulder in Baghosh, the scale is 20 cm long. This mollusc shells are applied for age determination

(*Vermetidae* and *Dendropoma*) on various surfaces. The long axis of the majority of boulders at this site is oriented to NW–SE.

Andalusia: situated about 3 km to the east of Marsa Matrouh, this stretch of the coast consists of a narrow, up to 50 m wide, low-lying rocky platform that ends at a higher platform 6–7 masl. Ten medium to very coarse boulders were documented here. Boulders accumulations consisted of mostly medium-sized boulders packed into imbricated clusters at a distance of 20 m from the shoreline. The landward limit of the boulder deposit is

marked by rise of the coastal platform. A number of coarse and very coarse boulders are found up to 6 m from the shoreline, and the shape and attached marine incrustations suggest a submerged origin for the largest of these boulders. Morphometric properties of the very coarse boulders are presented in Table 1. For about 90 % of the boulders, the long axes are oriented in a NW–SE direction.

4.2 Boulder statistics

The relationship between boulders weight and distance from shoreline for each site is plotted in Fig. 4. In Baghosh, a general landward fining trend in the size of the boulders is recognizable, with large boulders generally found up to 10 m from the shoreline. At Marazik, the largest boulders are found at a maximum distance of 30 m from the shoreline. At Hasheesh, most large boulders are found close the shoreline, but a very large boulder (Ha-20) is 40 m far from the shoreline. In Andalusia, large boulders are found up to 6 m from the shoreline, with only small and medium-sized boulders found up to 20 m from shoreline.

4.3 Storm and tsunami wave heights calculation

For hydrodynamic calculations, we only take into account the very coarse boulders with a major axis longer than 2 m. In line with observed conditions in the field, a submerged or joint-bounded pre-setting is presumed for each boulder. The calculated tsunami and storm wave height (at breaking point) capable of initiating transportation of each boulder is presented in Table 1.

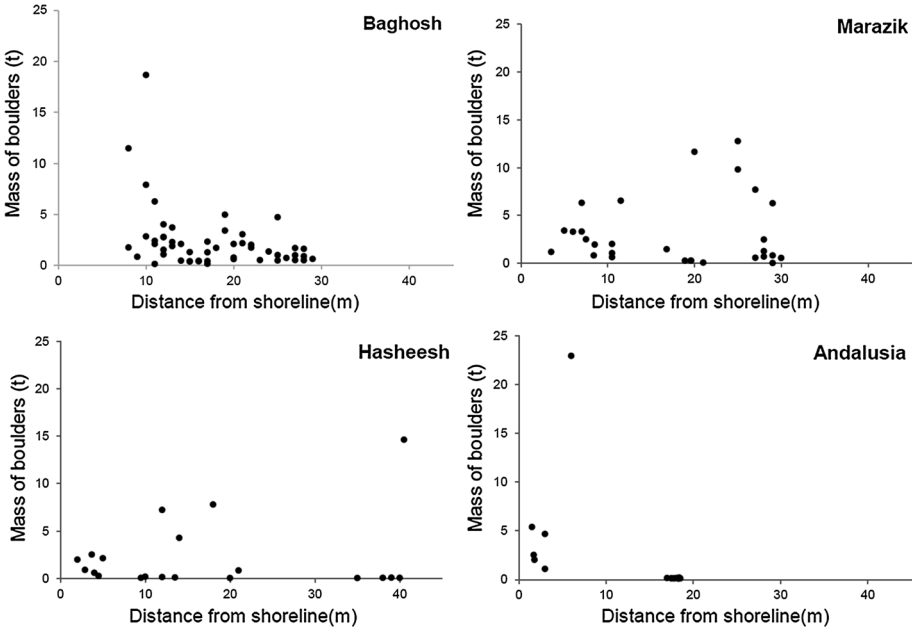

Fig. 4 Boulder mass plotted against distance from the coastline at the four study sites

4.4 Attached marine organisms and age determination

As stated above, some boulders have attached marine organisms from two fixed gastropod families: *Vermetidae* and *Dendropoma*. These marine encrustations are known as biological indicators for the upper part of the subtidal zone in the Mediterranean (Laborel, 1986; Murray-Wallace and Woodroffe, 2014; Rovere et al. 2015). These organisms live in distinct depths and have a short lifespan. As such, they can be used to determine the emergence time of individual boulders. *Vermetidae* and *Dendropoma* shells collected from four very coarse boulders were subjected to AMS radiocarbon dating in Poznan radiocarbon laboratory. Ages were calibrated using the marine 13.14C calibration curve (Reimer et al., 2013). Based on recent radiocarbon measurements on pre-bomb marine shells in the Levant Sea, the recommended ΔR of 52 ± 40 14C years was applied for calibration (Reimer and McCormac 2002). Results are presented in Table 2.

5 Discussion

According to the applied hydrodynamic models (Table 1), the displacement of the largest boulders could be initiated by (i) storm waves exceeding 10 m at breaking point or (ii) tsunami waves higher than 2.6 m. These hydrodynamic models only estimate the minimum wave heights capable of transporting the boulders but cannot answer the critical question of the nature and origin of the waves. Several studies have been devoted to developing criteria for distinguishing between tsunami- and storm-transported deposits (e.g. Goff et al. 2004; Anthony 2009; Goto et al. 2010; Paris et al. 2011; Engel and May 2012). However, discriminating between tsunami and storm boulders remains complicated since most of the characteristics are similar. Distinguishing criteria are mostly case dependent, and ambiguity remains in many cases. It is necessary to take into account multiple factors such as the geomorphology of the coast, the spatial distribution of boulders and the history of inundation events in order to evaluate the plausibility of a storm or tsunami origin.

In the Mediterranean, the rich historical literature is a key tool in investigations of inundation events. In the eastern region, detailed historical earthquake and tsunami catalogues are available (Guidoboni et al. 1994; Soloviev et al. 2000; Papadopoulos and Fokaefs 2005; Salamon et al. 2007; Papadopoulos et al. 2014). However, historical records of tsunamis in the coast of Egypt are less known compared to the northern coast. By reviewing the main historical records, it is apparent that at least six tsunamis impacted Alexandria and the Nile delta with the largest events generated by earthquakes greater than Mw 7 originating from the Hellenic arc (Table 3). The earthquake and tsunami of 365 AD

Table 2 Radiocarbon and calibrated ages of attached marine organism from four very coarse boulders

Boulder	Mass (t)	Dated biomarker	Site	14C Age	Calibrated age (2 δ range)
Ba-23	18.3	*Vermetidae*	Baghosh	1220 ± 30 BP	1118–1319 AD
Mr-27	12.8	*Dendropoma*	Marazik	450 ± 25 BP	Modern
Ha-20	14.6	*Vermetidae*	Hasheesh	545 ± 30 BP	1712–1949 AD
And-02	22.9	*Vermetidae*	Andalusia	515 ± 25 BP	1723–1949 AD

Table 3 Historical tsunamis reported for the Mediterranean coast of Egypt (Guidoboni et al. 1994; Soloviev et al. 2000; Salamon et al. 2007; Papadopoulos et al. 2014)

Date	Source	Reported in	Earthquake size	Tsunami extent
23 BC	?	Alexandria	?	Small
365 AD	Western Hellenic arc	Alexandria	Large (Mw $\geq$ 7)	Large
1303 AD	Eastern Hellenic arc	Alexandria	Very large (Mw $\geq$ 7.5)	Large
1759 AD	Levant coast	Nile delta	Large (Mw $\geq$ 7)	Small–moderate
1870 AD	Eastern Hellenic arc	Alexandria	Large (Mw $\geq$ 7)	Small–moderate
1908 AD	Messina (Sicily)	Alexandria	Large (Mw $\geq$ 7)	Small

affected a vast area in the eastern Mediterranean and had a strong impact on the Egyptian coast around Alexandria. It is reported that 50,000 people lost their lives in Alexandria (Stiros 2001, Pararas-Carayannis 2011; Mastronuzzi et al. 2013). The great earthquake and tsunami of 8 August 1303 AD also affected a large area of the eastern Mediterranean (Guidoboni et al. 1994; El-Sayed et al. 2000; Ambraseys 2009). The Mw $>$ 7.5 earthquake was generated near the east coast of Crete (Fig. 1). The most serious destruction was reported from north-eastern Crete where the tsunami struck the city of Heraklion. In Alexandria, large waves destroyed port facilities and damaged the great lighthouse, many houses were ruined and much of the city wall was destroyed (El-Sayed et al. 2000; Papadopoulos et al. 2010; 2014). Two large earthquakes occurred in October and November 1759 along the Dead Sea fault on the Levant coast, the tsunami associated with this event was probably generated by a submarine slump (Salamon et al. 2007). This tsunami has little impact on the Nile delta. After the Eastern Hellenic arc earthquake of 1870, a small tsunami was reported to have struck Alexandria and caused some damage to boats (Soloviev et al. 2000). A great earthquake in Messina (Sicily) in 1908 generated a tsunami that had minor impact on the coast of Egypt. A list of historical tsunamis reported from the Egyptian coast of the Mediterranean is presented in Table 3. Two events of 365 AD and 1303 AD are expected to associate with considerably high waves and vast inundation around Alexandria. According to frequent report of serious damage and causalities, considering the historical reports of damage to the city walls and inundation of thousand houses in Alexandria, a tsunami height of 5 to 6 m is plausible for the event of 1303 AD. Assuming a Mw 7.5 earthquake at a depth 10–15 km in the western Hellenic Arc, modelling indicates that tsunami wave heights of up to 5.7 m would have been experienced in Alexandria (El-Sayed et al. 2000). Such a tsunami would have been able to transport all of the boulders measured in this study. Geomorphological evidences for the 1303 AD tsunami are found in the eastern Mediterranean with Scheffers et al. (2008) reporting large displaced boulders in the southern Peloponnese (Greece), attached marine organisms on boulders yielded a calibrated radiocarbon age of around 1300 AD.

In this study, the age determination on the largest boulder (Ba-23) in the Baghosh site had an age range of 1118–1319 AD (Table 2). This age is broadly compatible with the great tsunami of 1303 AD. However, sharp edges and fresh surfaces on most of the medium-sized boulders at this site suggest a younger age. Multiple impacts of large waves over different time periods are a possibility that should be tested by further study and age determinations.

At three other sites, age determinations give range from the eighteenth century AD to present. Over this period, three far-field tsunamis are reported to have occurred along the coast of Egypt (1759 AD, 1870 AD and 1908 AD). However, the impact was at best moderate and there is no report of large waves or considerable inundation associated with these events.

The history of large storms is more ambiguous because of short and discontinuous instrumental records. Wave height measurements between 1985 and 2011 indicate that the maximum wave height recorded was 5.44 m at a water depth of 18 m along the west coast of Alexandria. Iskander (2013) used all available data to model extreme wave conditions for return periods of 50 and 100 years and produced wave heights of 7.6 and 8.1 m, respectively. While calculated at 18 m water depth, it is worth noting that wave heights at their breaking point would have been higher. Therefore, the largest probable storm over a 100-year interval would also most likely have had the potential to move most of the boulders reported in this study. Storms may well have been stronger in the past, and there is evidence for intense storminess in the Mediterranean during the Little Ice Age between the sixteenth and nineteenth centuries AD (e.g. Dezileau et al. 2011; Sabatier et al. 2012; Shah-Hosseini et al. 2013; Dezileau and Castaings 2014).

The distribution pattern is more likely to be controlled by the geomorphological characteristics of the boulders and the coastline rather than wave properties. Some recent field surveys suggest that tsunamis impart longer transport distances and produce a lower concentration of boulders than storms (e.g. Goto et al. 2007; Paris et al., 2009). In contrast though, Etienne et al. (2011) report imbricated packing, limited landward extent and the absence of landward fining for boulder deposits laid down by the 2004 Indian Ocean and 2009 South Pacific tsunamis. Goff et al. (2006) on the other hand observed landward fining pattern in tsunami boulders in Hawaii. In this study, a clear landward fining trend is recognizable at Baghosh and Andalusia with the larger boulders only found up to a maximum distance of 10 m from the shoreline (Fig. 4). In contrast, at Marazik and Hasheesh, a landward fining trend is absent and large boulders can be found up to 30–40 m inland with the maximum distance of boulder transport limited by a rise in the rocky platform (Fig. 2). The orientation of the long axis in the majority of boulders at three sites (Marazik, Hasheesh and Andalusia) is generally parallel to the N–NW direction of prevailing waves and winter storms. Only in Baghosh are most boulders oriented to E–W direction (Fig. 2). Considering the similarities in coastal geomorphology between all four of the study sites, the differences in ages, size and distribution pattern could may well be related to multiple events from different sources. A more detailed study and age determination of boulders may lead to a better understanding of the nature and properties of the transporting waves.

6 Conclusions

Coastal boulder accumulations along the Mediterranean coast of Egypt were investigated at four sites between Alexandria and Marsa Matrouh. The morphometric characteristics, spatial distribution and biological attachments indicate that the boulders were detached from the rocky coast or transported from an original submerged setting by the impact of large waves. Hydrodynamic calculations imply that the largest boulders could have initially been transported by a 2.6-m-high tsunami wave or by storm waves about 10 m high at their breaking point. According to historical records, a tsunami as large as the 1303 AD

event was capable of transporting all of the studied boulders to their final position. Storm wave height modelling also suggests a similar possible outcome. The age of the largest boulder from the easternmost section of the study area broadly coincides with that of the 1303 AD tsunami. After 1303 AD, there is no record of a similarly large tsunami within the study area. Three other ages, as well as the morphological properties of most boulders, suggest younger ages for boulder deposits ranging from the eighteenth century AD to present. We suggest that the boulder deposits are quite plausibly related to inundations associated with multiple extreme storms with wave heights exceeding 10 m at breaking point in last two centuries, possibly related to high storminess during the Little Ice Age. Although the hazard of extreme storms appears to be more probable over a short time period, the risk of tsunamis from large earthquakes mainly generated from the Hellenic arc or alternative regional sources cannot be neglected. More studies are necessary to constrain the ages and origin of these boulder deposits. This study points to the potential of extreme wave hazards along this heavily populated and rapidly developing part of the Mediterranean coast of Egypt. The vulnerability of this region must be considered in coastal risk assessments.

Acknowledgments This work is a joint Franco-Egyptian contribution to the research project IMHOTEP. It has been partially funded by the Egyptian Academy of Scientific Research and Technology, the University of Aix-Marseille (France), Faculty of Education of Ain-Shams University (Cairo) and ANR-GEOMAR funded by French National Center for Scientific Research (CNRS). This work has been carried out thanks to the support of the Labex OT-Med (ANR-11-LABX-0061) and of the AMIDEX project (n° ANR-11-IDEX-0001-02), funded by the "Investissements d'Avenir" French Government program, managed by the French National Research Agency (ANR). Authors wish to thank three reviewers for their constructive comments and Pr. James Goff from the University of New South Wales, Australia, for very useful comments and English corrections.

References

Ambraseys N (2009) Earthquakes in the eastern Mediterranean and the Middle East: a multidisciplinary study of seismicity up to 1900. Cambridge University Press, Cambridge

Anthony EJ (2009) Shore processes and their palaeoenvironmental applications. Developments in marine geology. Elsevier, Amsterdam

Anzidei M, Lambeck K, Antonioli F, Furlani S, Mastronuzzi G, Serpelloni E, Vannucci G (2014) Coastal structure, sea level changes and vertical motion of the land in the Mediterranean. In: Martini IP, Wanless HR (eds) Sedimentary coastal zones from high to low latitudes: similarities and differences. Geological Society, London **(special publications)**

Barbano MS, Pirrotta C, Gerardi F (2010) Large boulders along the south-eastern Ionian coast of Sicily: storm or tsunami deposits? Mar Geol 275:140–154

Benner R, Browne T, Brückner H, Kelletat D, Scheffers A (2010) Boulder transport by waves: progress in physical modelling. Z Geomorphol Supp 54:127–146

Biolchi S, Furlani S, Antonioli F, Baldassini N, Causon Deguara J, Devoto S, Di Stefano S, Evans J, Gambin T, Gauci R, Mastronuzzi G, Monaco C, Scicchitano G (2016) Boulder accumulations related to extreme wave events on the eastern coast of Malta. Nat Hazards Earth Syst Sci 16:737–756

Blair TC, McPherson JG (1999) Grain-size and textural classification of coarse sedimentary particles. J Sediment Res 69:6–19

Dawson AG (1994) Geomorphological effects of tsunami run-up and backwash. Geomorphology 10:83–94

Dezileau L, Castaings J (2014) Extreme storms during the last 500 years from lagoonal sedimentary archives in Languedoc (SE France). Méditerranée 122:113–119

Dezileau L, Sabatier P, Blanchemanche P, Joly B, Swingedouw D, Cassou C, Castaings J, Martinez P, Von-Grafenstein U (2011) Intense storm activity during the Little Ice Age on the French Mediterranean coast. Palaeogeogr Palaeocl 299:289–297

Eissa M (1994) On the cold season Squalls over North Egypt and their impact on desert development. Dissertation, Institute of Environmental Studies and Research, Ain-Shams University, Egypt

El-Sayed A, Romanelli F, Panza G (2000) Recent seismicity and realistic waveforms modeling to reduce the ambiguities about the 1303 seismic activity in Egypt. Tectonophysics 328:341–357

Embabi NS (2004) The geomorphology of Egypt (landform and evolution). The Egyptian Geographical Society, Cairo **(special publication)**

Engel M, May SM (2012) Bonaire's boulder fields revisited evidence for Holocene tsunami impact on the Leeward Antilles. Quat Sci Rev 54:126–141

Etienne S, Paris R (2010) Boulder accumulations related to storms on the south coast of the Reykjanes Peninsula (Iceland). Geomorphology 114:55–70

Etienne S, Buckley M, Paris R, Nandasena AK, Clark K, Strotz L, Chagué- Goff C, Goff J, Richmond B (2011) The use of boulders for characterizing past tsunamis: lessons from the 2004 Indian Ocean and 2009 South Pacific tsunamis. Earth Sci Rev 107:76–90

Frihy OE (2001) The necessity of environmental impact assessment (EIA) in implementing coastal projects: lessons learned from the Egyptian Mediterranean Coast. Ocean Coast Manag 44:489–516

Morhange C, Salomon A, Bony G, Flaux C, Galili, E, Goiran JP, Zviely D (2014) Geoarchaeology of tsunamis and the revival of neo-catastrophism in the Eastern Mediterranean. In: La Sapienza studies on the archaeology of palestine and transJordan, ROSAPAT 11:61-81, Rome, pp 31–50

Goff J, McFadgen BG, Chagué-Goff C (2004) Sedimentary differences between the 2002 Easter storm and the 15th-century Okoropunga tsunami, southeastern North Island, New Zealand. Mar Geol 204:235–250

Goff J, Liu PL, Higman B, Morton R, Jaffe BE, Fernando H, Lynett P, Fritz H, Synolakis C (2006) The December 26th 2004 Indian Ocean Tsunami in Sri Lanka. Earthq Spectra 22(S3):155–172

Goodman-Tchernov BN, Dey HW, Reinhardt EG, MacCoy F, Mart Y (2009) Tsunami waves generated by the Santorini eruption reached Eastern Mediterranean shores. Geology 37(10):943–946

Goto K, Chavanich SA, Imamura F, Kunthasap P, Matsui T, Minoura K, Sugawara D, Yanagisawa H (2007) Distribution, origin and transport process of boulders deposited by the 2004 Indian Ocean tsunami at Pakarang Cape, Thailand. Sediment Geol 202:821–837

Goto K, Miyagi K, Kawamata H, Imamura F (2010) Discrimination of boulders deposited by tsunamis and storm waves at Ishigaki Island, Japan. Mar Geol 269:34–45

Guidoboni E, Comastri A, Traina G (1994) Catalogue of ancient earthquakes in the Mediterranean area up to the 10th century. Istituto Nazionale di Geofisica, Rome **504 pp**

Hoffmeister D, Ntageretzis K, Aasen H, Curdt C, Hadler H, Willershäuser T, Bareth G, Brückner H, Vött A (2014) 3 D model-based estimations of volume and mass of high-energy dislocated boulders in coastal areas of Greece by terrestrial laser scanning. Z Geomorphol 58(Suppl 3):115–135

Imamura F, Goto K, Ohkubo S (2008) A numerical model for the transport of a boulder by tsunami. J Geophys Res 113:1–12

Iskander MM (2013) Wave climate and coastal structures in the Nile delta coast of Egypt. Emir J Eng Res 18(1):43–57

Laborel J (1986) Vermetid gastropods as sea-level indicators. In: van de Plassche O (ed) Sea-level research: a manual for the collection and evaluation of data. Geo Books, Norwich, pp 281–310

Lionello P, Bhend J, Buzzi A, Della-Marta PM, Krichak S, Jansa A, Maheras PA, Sanna A, Trigo IF, Trigo R (2006) Cyclones in the Mediterranean region: climatology and effects on the environment. In: Lionello P, Malanotte-Rizzoli P, Boscolo R (eds) Mediterranean climate variability. Elsevier, Amsterdam, pp 325–372

Maouche S, Morhange C, Meghraoui M (2009) Large boulder accumulation on the Algerian coast evidence tsunami events in the western Mediterranean. Mar Geol 262:96–104

Mastronuzzi G (2010) Tsunami in Mediterranean Sea. Egypt J Environ Change 2–1:1–9

Mastronuzzi G, Sansò P (2000) Boulders transport by catastrophic waves along the Ionian coast of Apulia (Southern Italy). Mar Geol 170:93–103

Mastronuzzi G, Sansò P (2004) Large boulder accumulations by extreme waves along the Adriatic coast of southern Apulia (Italy). Quat Int 120:173–184

Mastronuzzi G, Pignatelli C, Sansò P (2006) Boulder fields: a valuable morphological indicator of paleotsunami in the Mediterranean Sea. Z Geomorph NF Suppl 146:173–194

Mastronuzzi G, Pignatelli C, Sansò P, Selleri G (2007) Boulder accumulations produced by the 20th of February, 1743 tsunami along the coast of southeastern Salento (Apulia region, Italy). Mar Geol 242:191–205

Mastronuzzi G, Brückner H, De Martini PM, Regnauld H (2013) Tsunami: from the open sea to the coastal zone and beyond. In: Mambretti S (ed) Tsunami: from fundamentals to damage mitigation. WIT Press, Southampton, pp 1–36

McKenzie D (1972) Active tectonics of the Mediterranean region. Geophys J Int 30:109–185

Morhange C, Marriner N, Pirazzoli A (2006) Evidence of late-Holocene tsunami events in Lebanon. Z Geomorphol NF Suppl 146:81–95

Morton RA, Richmond BM, Jaffe BE, Gelfenbaum G (2006) Reconnaissance investigation of Caribbean extreme wave deposits; preliminary observations, interpretations and research directions. Open-File Report 2006–1293, US Geological Survey

Murray-Wallace CV, Woodroffe CD (2014) Methods of dating Quaternary sea-level changes. In: Murray-Wallace CV, Woodroffe CD (eds) Quaternary sea-level changes. Cambridge University Press, Cambridge, pp 131–186

Naffaa MG, Fanos AM, el Ganainy MA (1991) Characteristics of waves off the Mediterranean coast of Egypt. J Coast Res 7(3):665–676

Nandasena NAK, Paris R, Tanaka N (2011) Reassessment of hydrodynamic equations: minimum flow velocity to initiate boulder transport by high energy events (storms, tsunamis). Mar Geol 281:70–84

Nandasena NAK, Tanaka N, Sasaki Y, Osada M (2013) Boulder transport by the 2011 Great East Japan tsunami: comprehensive field observations and whither model predictions? Mar Geol 346:292–309

Noormets R, Crook KAW, Felton EA (2004) Sedimentology of rocky shorelines: 3. Hydrodynamics of megaclast emplacement and transport on a shore platform, Oahu, Hawaii. Sediment Geol 172:41–65

Nott J (1997) Extremely high-energy wave deposits inside the Great Barrier Reef, Australia: determining the cause—tsunami or tropical cyclone. Mar Geol 14:193–207

Nott J (2000) Records of prehistoric tsunamis from boulder deposits. Evidence from Australia. Sci Tsunami Hazard 18(1):1–14

Nott J (2003) Waves, coastal boulder deposits and the importance of pre-transport setting. Earth Planet Sci Lett 210:269–276

Papadopoulos GA, Fokaefs A (2005) Strong tsunamis in the Mediterranean Sea: a re-evaluation. ISET J Earthq Tech 42:159–170

Papadopoulos GA, Daskalaki E, Fokaefs A, Giraleas N (2010) Tsunami hazard in the Eastern Mediterranean Sea: strong earthquakes and tsunamis in the west Hellenic arc and trench system. J Earthq Tsunami 4:145–179

Papadopoulos GA, Gràcia E, Urgeles R, Sallares V, De Martini PM, Pantosti D, González M, Yalciner AC, Mascle J, Sakellariou D, Salamon A, Tinti S, Karastathis V, Fokaefs A, Camerlenghi A, Novikova T, Papageorgiou A (2014) Historical and prehistorical tsunamis in the Mediterranean and its connected seas: geological signatures, generation mechanisms and coastal impacts. Mar Geol 354:81–109

Pararas-Carayannis J (2011) The earthquake and tsunami of July 21, 365 AD in the eastern Mediterranean Sea, review of impact on the Ancient World, assessment of recurrence and future impact. Sci Tsunami Hazard 30–4:253–294

Paris R, Wassmer P, Sartohadi J, Lavigne F, Barthomeuf B, Desgages E, Grancher D, Baumert P, Vautier F, Brunstein D, Gomez C (2009) Tsunamis as geomorphic crisis: lessons from the December 26, 2004 tsunami in Lhok Nga, west Banda Aceh (Sumatra, Indonesia). Geomorphology 104:59–72

Paris R, Naylor LA, Stephensonc WJ (2011) Boulders as a signature of storms on rock coasts. Mar Geol 283(1–4):1–11

Pignatelli C, Sansò P, Mastronuzzi G (2009) Evaluation of tsunami flooding using geomorphologic evidence. Mar Geol 260(1–4):6–18

Raji O, Dezileau L, Von Grafenstein U, Niazi S, Snoussi M, Martinez P (2015) Extreme sea events during the last millennium in the northeast of Morocco. Nat Hazards Earth Syst Sci 15:203–211

Reimer PJ, McCormac FG (2002) Marine radiocarbon reservoir corrections for the Mediterranean and Aegean Seas. Radiocarbon 44:159–166

Reimer PJ, Bard E, Bayliss A et al (2013) IntCal13 and Marine13 radiocarbon age calibration curves 0–50,000 years cal BP. Radiocarbon 55(4):1869–1887

Rovere A, Antonioli F, Bianchi CN (2015) Fixed biological indicators. In: Shennan I, Long AJ, Horton BP (eds) Handbook of sea-level research. Wiley, Chichester, pp 268–280

Sabatier F, Dezileau L, Colin C, Briqueu L, Bouchette F, Martinez P, Siani G, Rayna O, Von-Grafenstein U (2012) 7000 Years of paleostorm activity in the NW Mediterranean Sea in response to Holocene climate events. Quat Res 77:1–11

Salamon A, Rockwell T, Ward SN, Guidoboni E, Comastri A (2007) Tsunami hazard evaluation of the eastern Mediterranean: historical analysis and selected modelling. Bull Seismol Soc Am 97(3):705–724

Scheffers A, Kelletat D, Vött A, May SM, Scheffers S (2008) Late Holocene tsunami traces on the western and southern coastlines of the Peloponnesus (Greece). Earth Planet Sci Lett 269:271–279

Scicchitano G, Monaco C, Tortorici L (2007) Large boulder deposits by tsunami waves along the Ionian coast of south-eastern Sicily (Italy). Mar Geol 238:75–91

Shah-hosseini M, Morhange C, Naderi Beni A, Marriner N, Lahijani H, Hamzeh M, Sabatier F (2011) Coastal boulders as evidence for high-energy waves on the Iranian coast of Makran. Mar Geol 290:17–28

Shah-Hosseini M, Morhange C, De Marco A, Anthony EJ, Sabatier F, Mastronuzzi G, Pignatelli C, Piscitelli A (2013) Coastal boulders in Martigues, French Mediterranean: evidence for extreme storm waves during the Little Ice Age. Z Geomorphol 57(4):181–199

Soloviev SL, Solovieva ON, Go CN, Kim KS, Shchetnikov NA (2000) Tsunamis in the Mediterranean Sea 2000 BC–2000 AD. Kluwer Academic Publishers, Dordrecht

Stewart IS, Morhange C (2009) Coastal geomorphology and sea-level change. In: Woodward JC (ed) The Physical Geography of the Mediterranean. Oxford University Press, Oxford, pp 385–413

Stiros SC (2001) The AD 365 crete earthquake and possible seismic clustering during the fourth to sixth centuries AD in the Eastern Mediterranean: a review of historical and archaeological data. J Struct Geol 23(2):545–562

Switzer AD, Burston JM (2010) Competing mechanisms for boulder deposition on the southeast Australian coast. Geomorphology 114:42–54

Torab M, Dalal N (2015) Natural hazards mapping of mega sea-waves on the NW coast of Egypt. J Afr Earth Sci 112:353–357

Vacchi M, Rovere A, Zouros N, Firpo M (2012) Assessing enigmatic boulder deposits in NE Aegean Sea: importance of historical sources as tool to support hydrodynamic equations. Nat Hazard Earth Syst Sci 12:1109–1118

Vött A, Lang F, Bruckner H, Gakipapanastassiou K, Maroukian H, Papanastassiou D, Giannikos A, Hadler H, Handl M, Ntageretzis K, Willershäuser T, Zander A (2010) Sedimentological and geoarchaeological evidence of multiple tsunamigenic imprint on the Bay of Palairos-Pogonia (Akarnania, NW Greece). Quat Int 242(1):213–239